International Journal of Offshore and Coastal Engineering
Vol.8 | No. 2 | pp. 108 - 116 | November 2024
e-ISSN: 2580-0914

Submitted: February 9, 2024 | Revised: 28 April, 2024 | Accepted: June 6, 2024

Burst Pressure Analysis on Corroded Pipeline Using Finite Element Method

Mahadi Yahya Sormin[a*], Yoyok Setyo Hadiwidodo[a] and Nur Syahroni[a]

[a)] Department of Ocean Engineering, Institut Teknologi Sepuluh Nopember, Surabaya, Indonesia
*Corresponding author: mahadi.yahya.s@gmail.com

ABSTRACT

The oil and gas industry includes exploration, extraction, production or processing, and transportation. One of the important activities in the oil and gas industry is the hydrocarbon transportation system. The most commonly used hydrocarbon transportation facility is the subsea pipeline. Pipes operating in a marine environment can easily corrode. Corrosion will cause a metal loss on the pipe surface and worsen the strength of the pipe. The thinning of the pipe surface due to corrosion will result in localized holes of varying depths and uneven shapes on the outer and inner surfaces. A burst pressure will occur if the internal pressure in the pipe with corrosion defects exceeds the allowable internal pressure limit. Therefore, to prevent burst pressure, it is necessary to evaluate the residual strength of the pipe in order to determine whether the defective pipe with working pressure can continue to operate safely or not. The internal pressure value calculation results are as follows: until the pipe fails, it is considered to burst using an FEA of 19.42 MPa. Meanwhile, the internal pressure value using standard codes DNV-RP-F101 is 18.76 MPa. For the effect of variations in the dimensions of the corrosion defect size, the most influential is the length and depth of the defect due to a decrease in the graph that does not fluctuate. The percentage differences between the failure pressure values resulting from rectangle and semi-ellipsoidal corrosion defects and the burst pressure values from the burst test experiments are 0.61% and 0.15%, respectively.

Keywords: *Corroded Pipeline, Internal Pressure, Burst Pressure, Burst Capacity,*

1. INTRODUCTION

The world's energy needs continue to increase every year. A system is needed to exploit the mineral resources to meet these energy needs. The oil and gas industry includes exploration, extraction, production or processing, and transportation. Due to limited resources, petroleum exploration is carried out in land areas (onshore) and offshore areas (offshore). One of the important activities in the oil and gas industry is the hydrocarbon transportation system. Hydrocarbon transportation facilities that are commonly used are underwater pipelines or offshore pipelines.

Subsea pipelines greatly contribute to operating costs (OPEX). Failure of subsea pipelines can lead to catastrophic disasters that endanger the lives of people working in the environment. It can also cause environmental pollution and destabilize the underwater ecosystem. The company will suffer economic losses if the subsea pipeline fails [1].

Pipes operating in a marine environment can easily corrode. However, in the design stage of the pipeline estimating corrosion prevention methods such as adding cathodic protection, this protection may deteriorate over time. Corrosion will cause a metal loss on the pipe surface and worsen the strength of the pipe. It will result in the thinning of the pipe walls. Moreover, it will result in localized holes of varying depth and uneven shape on the outer and inner surfaces of the pipe. These localized holes are called corrosion defects. A burst pressure will occur if the internal pressure in the pipe with corrosion defects exceeds the allowable internal pressure limit. Burst pressure can be defined as the internal stress associated with the ligament remaining from the corroded area that exceeds the strain hardening level of the steel pipe and results in local fracture [2]. Therefore, to prevent burst pressure, it is necessary to evaluate the residual strength of the pipe to determine whether the pipe that has corrosion defects with working pressure can continue to operate safely or not.

2. LITERATURE REVIEW

One of the problems in maintaining the integrity of the pipe strength is corrosion. As a result of corrosion, subsea pipelines experience thinning of the walls' lining, causing defects. Therefore, an accurate evaluation is needed for safe pressure to pass through a pipe with defects due to corrosion. It is very important for the pipeline integrity management program concerning corrosion.

Several semi-empirical approach models have been carried out in industrial pipelines to evaluate burst pressure

on corroded pipes, such as ASME B31G, DNV RP F-101, CSA, RSTRENG, and PCORRC. However, this approach model has a relatively large model uncertainty due to assumptions and simplifications that reduce accuracy in predicting burst pressure (Bao et al., 2018). Among these methods, DNV-RP-F101 is the code most comprehensive and allows a relatively accurate average estimate of the residual strength of pipes that corrode when subjected to internal stresses [1].

Finite Element Analysis (FEA)) elastic-plastic three-dimensional. It has proven to be an effective tool for evaluating the burst capacity of corroded pipes. Although naturally occurring corrosion defects are irregular in shape, the corrosion defects considered in FEA are often modelled as rectangular 3D defects, which is the most conservative idealization of naturally occurring defects [2]. In the research of Mokhtari and Melchers comparing rectangular and semi-ellipsoidal corrosion defect models with the same depth of the defect, defect length, and width of the defect resulting in a semi-ellipsoidal model having an average margin of error of 5% and a rectangular defect model has an average margin of error of 11% in predicting the burst pressure value which is validated through a laboratory specimen test or full-scale burst test [3].

3. RESEARCH METHODOLOGY.

3.1 Data Collection

The process of collecting pipeline data in the form of pipe design properties data such as pipe length, outer pipe diameter, and pipe thickness follows. First, Pipe material data is also needed to determine the Elasticity Modulus (E), Yield Stress, and Ultimate Tensile Strength (UTS), which will later be needed to find the residual stress value. Defect dimension data on corroded pipe, such as defect length, width, and depth, are needed to find value *burst pressure*. The data used in this final project is test data from the experimental results *of the burst test* from the journal "An Experimental Investigation of the Effect of Defect Shape and Orientation on the Burst Pressure of Pressurized Pipes" quoted from the Journal of Al-Owaisi *et al.* (2018) [4].

Table 1 Pipe dimension and material characteristics [4]

Test Case No.	Steel Grade	Defect Type
1	X60	Rectangular

OD (mm)	ID (mm)	t (mm)	Specimen Length (mm)
508	490.2	8.9	1800

E (GPa)	σy (MPa)	σEng.uts (MPa)	σTrue.uts (MPa)
171	478	560	636

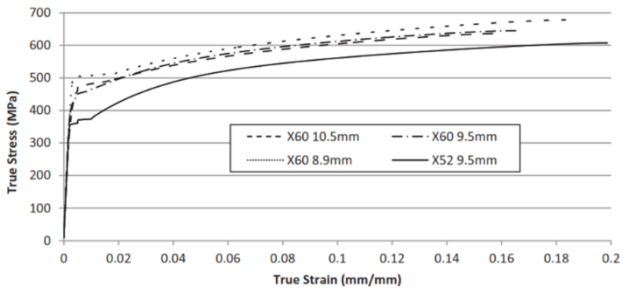

Figure 1 Stress-Strain Relationships [4]

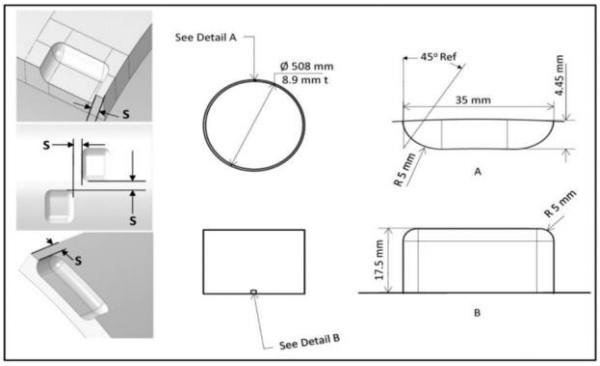

Figure 2 Characterized rectangle pitting corrosion details [4]

Table 2 Defect Size Based on Burst Test Experiment [4]

Test Case	I (mm)	w (mm)	d (mm)	P test (Mpa)
1	35	35	4.45	19.54

3.2 Failure Criterion

Failure pressure on a subsea pipeline can be defined as a failure due to the pressure that occurs where the pipe will leak or burst. It is necessary to consider the burst pressure that occurs to prevent failure due to internal pressure. The failure criterion used in this final project is the stress-based criterion.

The selection of failure criteria using a stress-based criterion follows the standard code of ASME B31.4 and ASME B31.8, which is calculated based on pressure criteria by considering various assumptions such as isotropic pressure in the plane, linear elastic, and homogeneous material. The standard code DNV-RP-F101 also uses a stress-based approach or Allowable Stress Design.

The criteria for plastic failure are events where the value of the von Mises pressure on the corrosion defect section touches the post-yield point of the material or the pressure that occurs around the thickness of the pipe wall in the corrosion defect section reaches the Ultimate Tensile Stress value, causing pipe failure.

In post-processing, Finite Element Analysis using ABAQUS, the von Mises stress distribution for the model can be represented by a stress contour that can explain the variation of the overall simulation results to determine the model failure zone and the stress value in that area.

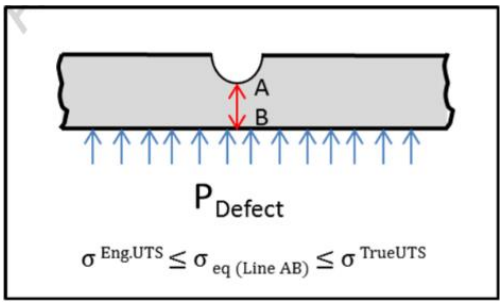

Figure 3 Failure Criteria [5]

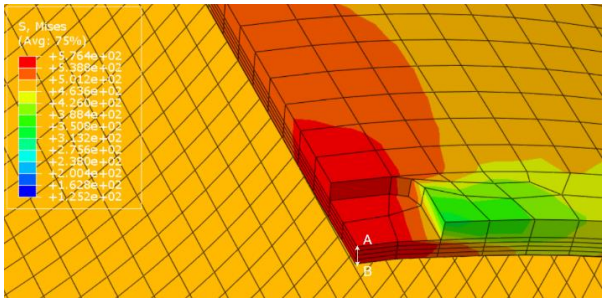

Figure 4 A-B Line Failure Criteria for Corrosion Defects

3.3 Load and Boundary Condition

In this process, the type of load to be carried out and its boundary conditions must be determined. In this final project, mechanical loads in the form of internal pressure are used. In addition, the load section can also input *Boundary Conditions* as the limits set in the ABAQUS CAE 2017 modelling. *Boundary Condition* inputs will be shown in the image below.

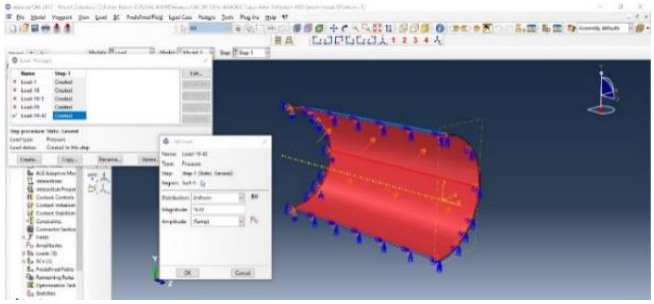
Figure 5 Applied Internal Pressure Load

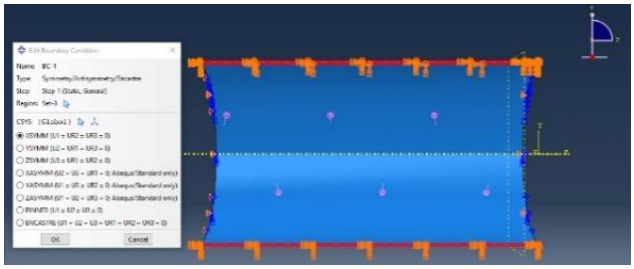
Figure 6 Boundary Condition Symmetrical on the X-axis

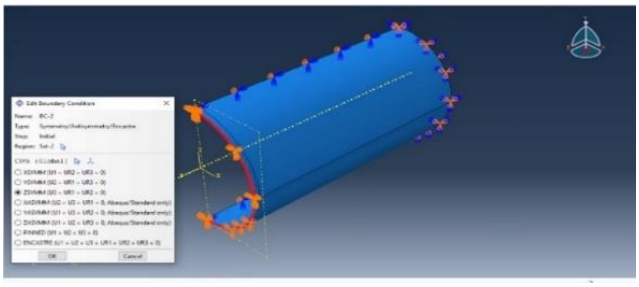
Figure 7 Boundary Condition Symmetrical on the Z-axis

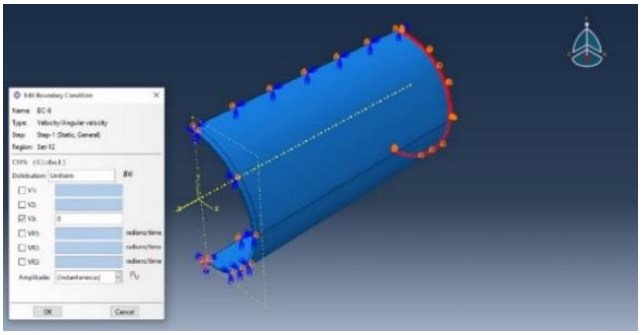
Figure 8 Boundary Condition Uz = 0 to prevent contraction expansion

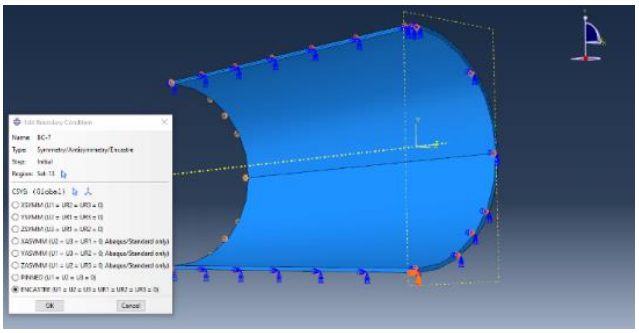
Figure 9 Fixed Boundary Condition on one node to prevent rigid body motion

3.4 Meshing sensitivity

This meshing sensitivity analysis was done by varying the density of different meshing sizes to the *equivalent stress von Mises value* to obtain the optimal mesh size. For this analysis of *meshing sensitivity*, 15 variations were carried out with densities ranging from 45 mm to 10 mm with C3D8R element types or eight hexahedral nodes. The graph below compares the number of elements and the percentage difference in *equivalent stress von Mises.*

Table 3 Mesh Sensitivity

Mesh Sensitivity				
Meshing Size (mm)	**Node**	**Element**	**Von Mises Stress at Node 21 (MPa)**	**Difference (%)**
45	2900	2195	561.139	-
40	3324	2529	562.635	0.27%
35	4246	3267	561.904	0.13%
30	5568	4329	567.467	0.99%
28	6450	5084	568.865	0.25%
26	7248	5689	567.792	0.19%
24	8490	6689	569.033	0.22%
22	9390	7414	570.765	0.30%
20	11760	9349	572.193	0.25%
15	20448	16449	575.194	0.52%
14	22698	18284	575.905	0.12%
13	26982	21809	576.116	0.04%

.

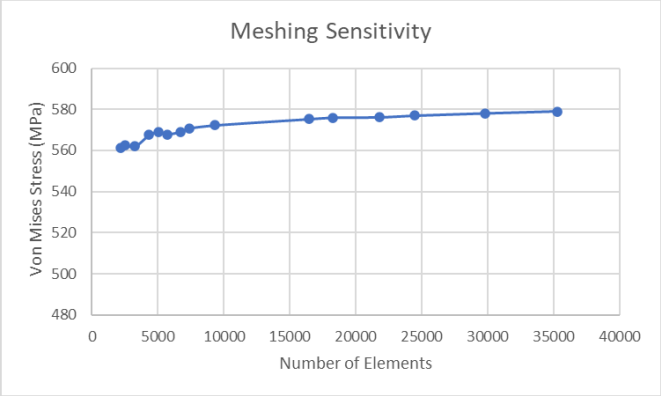

Figure 10 Mesh Sensitivity Graphic

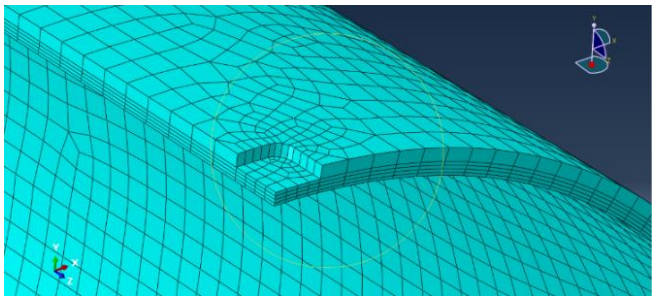

Figure 11 8-Node Hexahedral Element (C3D8R)

3.5 Methodology in determining the value of Burst pressure

The distribution of stress values that occur around the pipe can be seen through the simulation results of the finite element method model. In the non-linear analysis process, the load will increase with gradual changes, and the stress will also increase along with the increment process for each step. These results can be studied from the results of the Equivalent Stress Chart by reviewing the distribution of stress values by combining pipe failure criteria to evaluate whether the pipe has failed to burst pressure.

For example, the change in status for the value of the Equivalent Stress of corroded pipe on X60 pipe with a corrosion defect length of 35 mm, a defect depth of 4.45 mm, and a defect width of 35 mm with different pressure effects is shown in Figure 13 – Figure 16. The pressure used has an interval of 0.5 MPa. The pressures are 18 MPa, 18.5 MPa, 19 MPa, and 19.5 MPa.

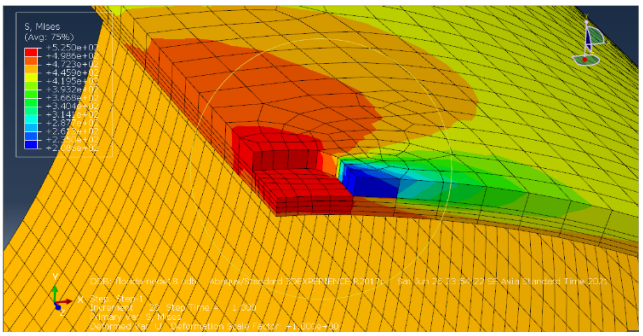

Figure 12 Von mises stress at 18 MPa

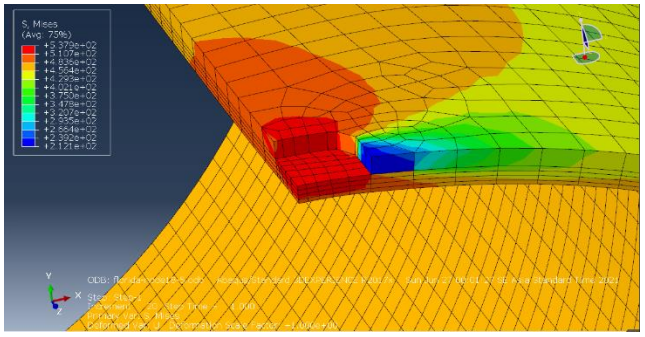

Figure 13 Von Mises stress at 18.5 Mpa

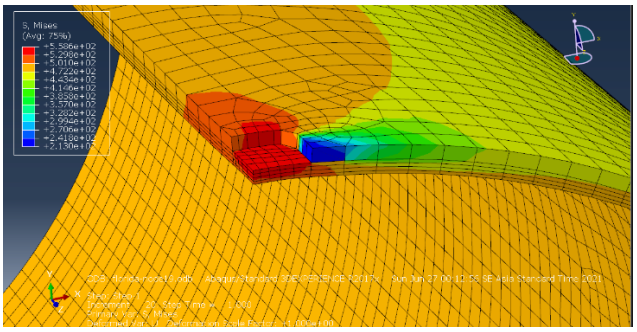

Figure 14 Von Mises stress at 19 MPa

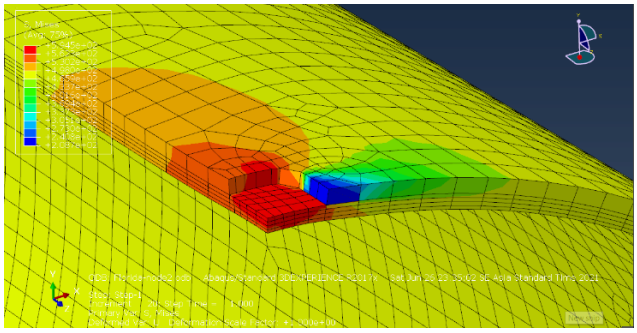

Figure 15 Von Mises Stress at 19.5 Mpa

The results show that the distribution of stress values in the corroded area is at different scales by increasing the pressure gradually until the pipe model fails according to its failure criteria. The stress gradually extends from the outside to the inside of the corroded area along the wall thickness. It can be seen that the value of S.Mises from Element ID 58115 changes from a pressure of 18 MPa with a value of S.Mises 524,293 MPa to 594,337 MPa at a pressure of 19.5 MPa.

3.6 Single Defects Failure Pressure calculation using DNV-RP-F101

The allowable stress approach is a safety criterion calculated based on the allowable stress design (ASD) without considering the element of uncertainty when calculating the failure pressure of the subsea pipeline.

$$P_f = \frac{2t\sigma_u(1-\frac{d}{t})}{(D-t)(1-\frac{d}{tQ})} \quad 3.1$$

Where:

$$Q = \sqrt{1+0{,}31\,(\frac{l}{\sqrt{Dt}})^2} \quad 3.2$$

P_f= *Burst Pressure* (MPa)(N/mm²)
d= depth defect (mm)
l= length defect (mm)
D= pipe diameter (mm)
t= Wall thickness (mm)
σ_u= initial design Specified Minimum Tensile Strength (MPa)(N/mm²)
Q= Length Correction Factor

The formula for calculating safe working pressure :

$$P_{sw} = FP_f \quad 3.3$$

Where :
P_{sw} = Safe working pressure (MPa) (N/mm²)
F = Total Usage Factor (F_1 x F_2)
F_1 = 0.9 (Modeling Factor)
F_2 = design Factor

4 RESULT AND DISCUSSION

4.1 Failure pressure value for characterized rectangle pitting corrosion

Perform simulations for corrosion defect conditions with rectangle-shaped using ABAQUS CAE 2017 to find the failure pressure value until the pipe fails. The value of the Finite Element Analysis of the internal pressure until the pipe fails on the X60 pipe is 19.42 MPa.

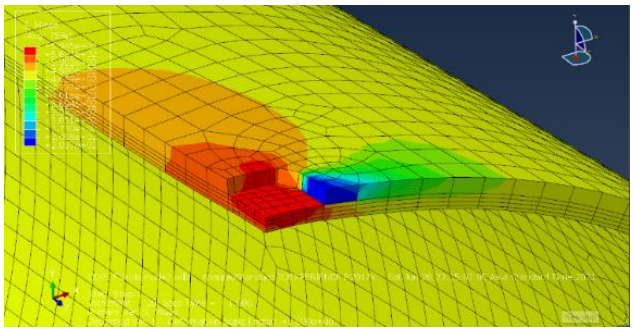

Figure 16 Characterized rectangle pitting corrosion Failure pressure value is 19.42 Mpa

By reviewing the value of the von Mises stress at each node that has been determined in the figure, namely on the y-axis area or against the wall thickness and also on the x-axis or in the circumferential direction, it can be seen that the value of the distribution of the equivalent stress von Mises stress on the corrosion defect rectangle. Due to the geometrical model being modelled in this study as a symmetrical quarter model, the value of the stress distribution at the node under consideration is right in the area under the core of the corrosion defect in the circumferential direction.

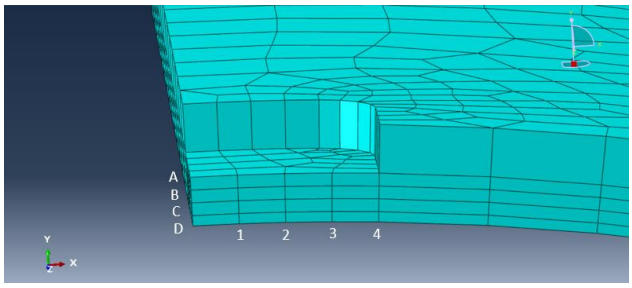

Figure 17 Reference Node Points

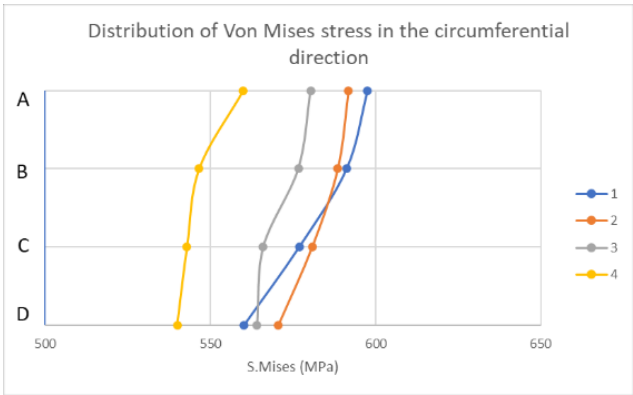

Figure 18 Distribution of Von Mises Stress in the circumferential direction

The value of the stress distribution of each node to be reviewed is shown in the figure, namely in the y-axis area or to the wall thickness, and also to the z-axis or the longitudinal direction can be seen the value of the equivalent stress distribution of von Mises stress on corrosion defects rectangle.

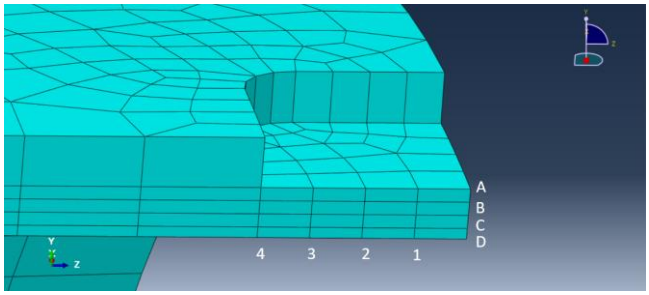

Figure 19 Reference Node Points

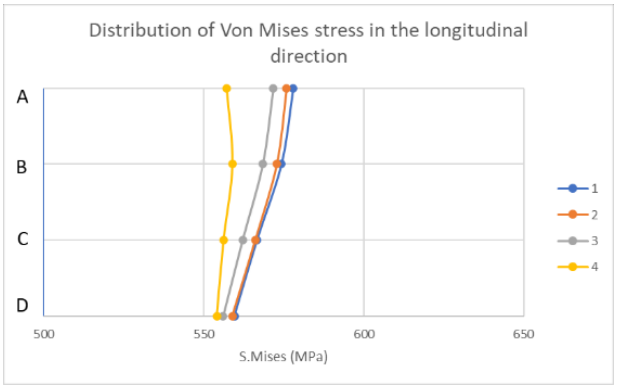

Figure 20 Distribution of Von Mises stress in the longitudinal direction.

This analysis found that the highest von Mises stress distribution was at Node A-1 towards the circumferential direction. It shows that the value of the von Mises stress distribution is centred just below the centre area of the corrosion defect. The value of the von Mises stress also decreases as it approaches the internal depth of the pipe and away from the centre of the corrosion defect.

4.1 Failure pressure calculation using DNV-RP-F101

$$Q = \sqrt{1 + 0{,}31\left(\frac{35}{\sqrt{(508)(8.9)}}\right)^2} = 1.041$$

$$P_f = \frac{2(8.9)(546.8)\left(1 - \frac{4.45}{8.9}\right)}{(508 - 8.9)\left(1 - \frac{4.45}{(8.9)(1.041)}\right)} = 18.76\ MPa$$

Safe Working Pressure value :

$P_{sw} = (0.9)(0.72) \times (18.76) = 12.15$ Mpa

4.2 Validation results

The model used in this final project is validated by comparing the predicted failure pressure value using Finite Element with the failure pressure value from the burst test experiment. In addition, the value of the finite element is also compared with the results of calculations using standard codes DNV RP F-101.

Table 4 Validation results

Reference Experimental Brust Pressure (Mpa)	FEA Failure Pressure (Mpa)	DNV Failure Pressure (Mpa)
19.54	19.42	18.76

Percentage difference (%)		
Reference Experimental Brust Pressure and FEA	**Reference Experimental Brust Pressure and DNV**	**DNV and FEA**
0.61	3.99	3.39

4.3 Variations in the width of the corrosion defect model

Studying the relationship of changes in the width of the corrosion defect to the value of the *burst pressure* by changing the width parameters such as 10.5 mm (0.6 w_0), 14 mm (0.8 w_0), 17.5 mm (w_0), 21 mm (1.2 w_0), 24.5 (1.4 w_0), 28 mm (1.6 w_0). Other parameters such as length and depth of defects remain the same, namely length of 35 mm and depth of 4.45 mm with Outside Diameter of 508 and Wall thickness of 8.9 mm.

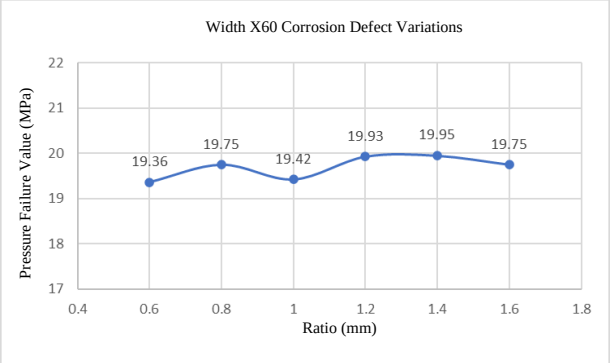

Figure 21 Relationship between the change of the defect width and the burst pressure

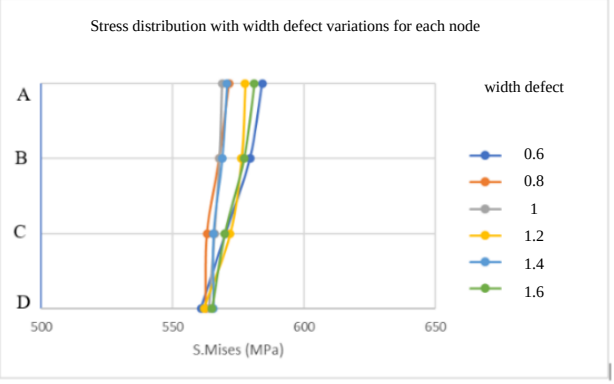

Figure 22 Distribution of Von Mises stress as a result of changing width defect

4.4 Variations in the length of corrosion defect model

Studying the relationship of changes in the width of corrosion defects to the value of *burst pressure* by changing width parameters such as 21 mm (0.6 l_0), 28 mm (0.8 l_0), 35 mm (l_0), 42 mm (1.2 l_0), 49 (1.4 l_0), 56 mm (1.6 l_0). Other parameters such as length and depth of defects remain the same, namely width of 17.5 mm and depth of 4.45 mm with an Outside Diameter of 508 and Wall thickness of 8.9 mm.

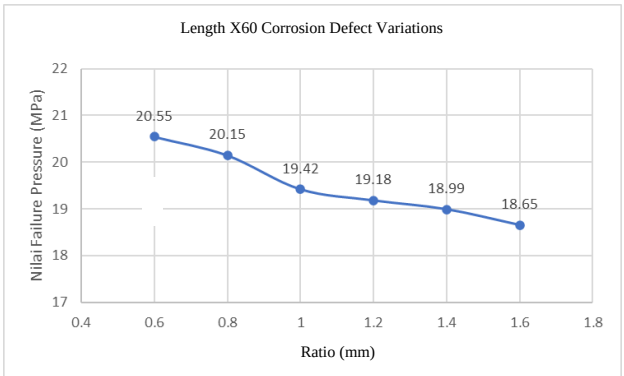

Figure 23 Relationship between the change of the length defect and the burst pressure

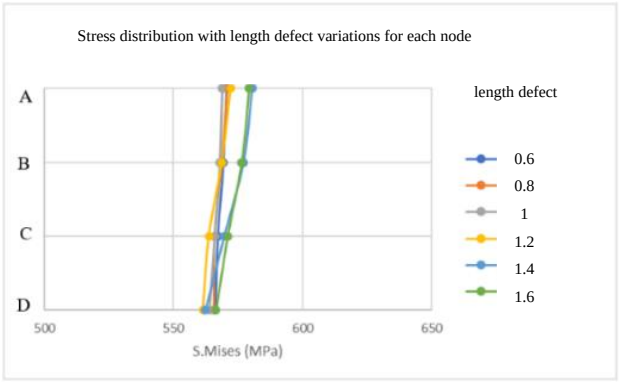

Figure 24 Distribution of Von Mises stress as a result of changing length defect

4.5 Variations in depth of the corrosion defect model

Studying the relationship of changes in the width of the corrosion defect to the value of the *burst pressure* by changing the width parameters such as 2.67 mm (0.6 d_0), 3.56 mm (0.8 d_0), 4.45 mm (d_0), 5.34 mm (1.2 d_0), 6.23 (1.4 s_0), 7.12 mm (1.6 s_0). Other parameters such as length and depth of defects remain the same, namely length of 35 mm and width of 17.5 mm with an Outside Diameter of 508 and a Wall thickness of 8.9 mm.

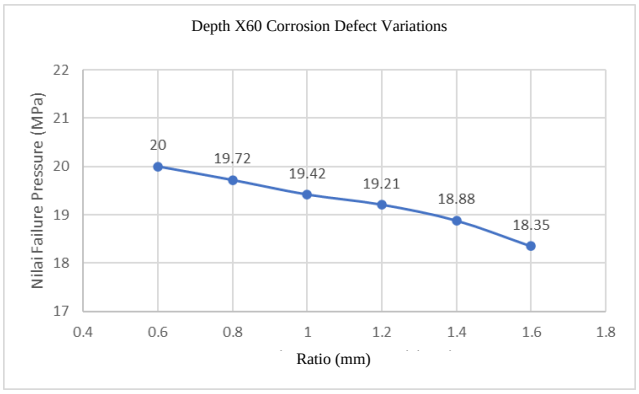

Figure 25 Relationships between the change of the defect depth and the burst pressure

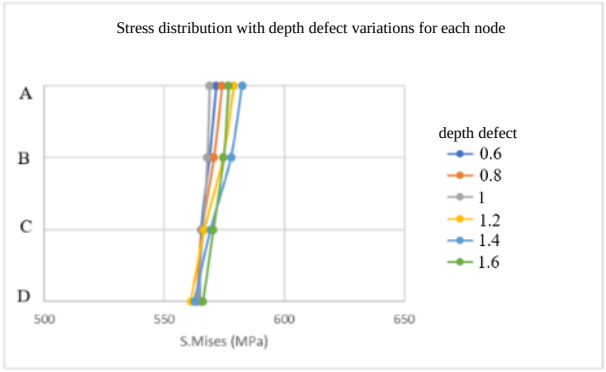

Figure 26 Distribution of Von Mises stress due to changing depth defect.

4.7 Comparison of burst pressure results from rectangular and semi-ellipsoidal pitting corrosion features

Simulations for corrosion defect conditions with semi-ellipsoidal shape were performed using ABAQUS CAE 2017 to find the value of the *failure pressure* until the pipe fails. The processing steps are the same as those for *finite element analysis* for rectangular corrosion defects. However, the semi-ellipsoidal corrosion defect section uses a 4-node linear tetrahedron or C3D4 element. The finite element analysis value until the pipe fails under internal pressure is 19.51 MPa.

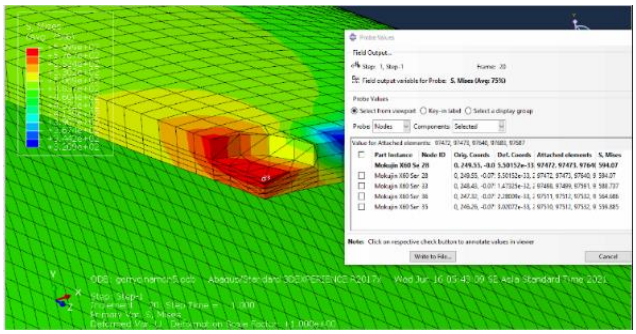

Figure 27 Semi-ellipsoidal defect failure pressure value is 19.51 MPa

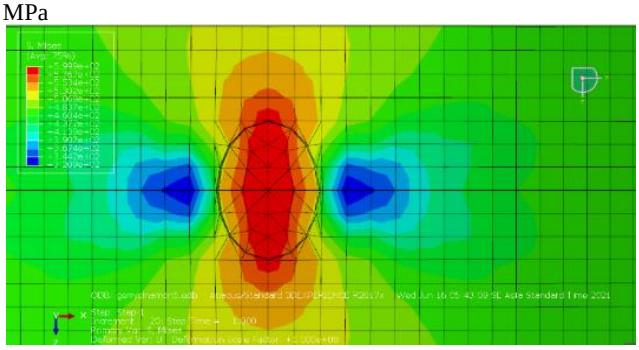

Figure 28 Semi-ellipsoidal corrosion defect

Table 5 Comparison of failure pressure value between the rectangle and semi-ellipsoidal corrosion defects idealization

FEA Failure Pressure Rectangle (Mpa)	FEA Failure Pressure Semi Elipsodial (Mpa)	DNV Failure Pressure Model (Mpa)
19.42	19.51	18.76

Percentage difference (%)		
FEA Complex-shaped and FEA Rectangle	**FEA Complex-Shaped and FEA Semi-elipsodial**	**DNV Model and FEA Complex-shaped**
0.56	0.10	3.94

4.8 Comparison of the failure pressure values for rectangle and semi-ellipsoidal corrosion defects idealization with complex-shaped defects

Corrosion defects that occur as natural equivalents are uneven in shape and irregularly distributed. Using geometry modelling of *pitting corrosion* simplified to estimate the capacity *burst pressure* still raises several questions. The first question is whether the simplified defect model is accurate concerning complex and realistic corrosion defects. Therefore, this study tries to answer this problem by comparing the results of *burst pressure* with simplified geometry of corrosion defects and corrosion defects of complex shapes using the same aspect ratio as rectangular and semi-ellipsoidal. Furthermore, the results of the complex-shaped corrosion defect model were used to investigate the accuracy of the simplified corrosion defect model.

Irregular holes were made with Autodesk Inventor 2019, and then *finite element analysis* was performed to find the failure pressure value using ABAQUS CAE 2017. The failure pressure value for Complex-shaped corrosion defects is 19.53 MPa.

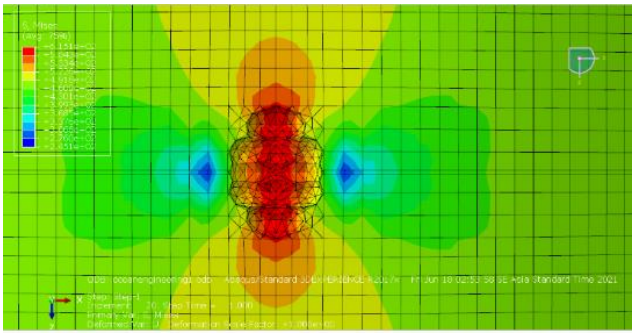

Figure 29 Complex-shaped corrosion defect

Determining how much the difference in metal volume is lost is appropriate to validate whether the complex-shaped corrosion defect model has a rectangle corrosion defect. The difference in the results of the volume of metal lost from complex-shaped corrosion defects with rectangle corrosion defects is 9.70%.

Table 6 Volume of metal lost differences from complex shaped corrosion defects and rectangle corrosion defects

	Area (mm^2)	Area (mm^3)
Complex Shaped Defect	1096.862	4881.036
Rectangle	1214.645	5405.170
Difference	9.70%	9.70%

The percentage difference in the failure pressure value from the Finite Element Analysis between rectangle corrosion defects and Complex-shaped defects is 0.56%. In comparison, for semi-ellipsoidal corrosion defects and Complex defects, it is 0.10%.

Table 7 Percentage difference between corrosion defects with simplified geometry and complex-shaped corrosion defects

FEA Failure Pressure Complex-Shaped (Mpa)	FEA Failure Pressure Rectangle (MPa)	FEA Failure Pressure Semi-elipsodial (MPa)	DNV Failure Pressure Model (MPa)
19.53	19.42	19.51	18.76

Percentages Difference (%)		
FEA Complex-shaped and FEA Rectangle	FEA Complex-shaped and FEA Semi-elipsodial	DNV Model and FEA Complex-shaped
0.56	0.10	3.94

5. CONCLUSION

Some conclusions that can be drawn from the analysis process that has been carried out are as follows:

1. The results of calculating the internal pressure value to the Von Mises equivalent stress meet the failure criteria, and the pipe is considered to burst using the finite element method of 19.42 MPa. Meanwhile, the internal pressure value using standard codes DNV-RP-F101 is 18.76 MPa.
2. For the analysis of the effect of variations in the size of corrosion defects, such as the width of the defect, the length of defect, and the depth of the defect, the most influential of the three variations of the dimensions of the corrosion defect are the length of the defect and the depth of the defect. The graph results show a steady decrease in internal pressure when the ratio of the dimensions of the length and width of the defect increases, causing the pipe to fail. In comparison, the results of the graph of the variation of the width of the internal pressure defect required for the pipe to fail are still unstable (fluctuating) when the ratio of the dimensions of the width of the corrosion defect increases.
3. The percentage difference in the failure pressure values from the finite element analysis resulting from rectangle and semi-ellipsoidal corrosion defects to the burst pressure values from the burst test experiment is 0.61% and 0.15%, respectively. In contrast, the percentage difference between the failure pressure values from the rectangle and semi-ellipsoidal corrosion defects and the failure pressure values from complex-shaped defects is 0.56% and 0.10%, respectively. These results show that the semi-ellipsoidal corrosion defect geometry approach has a smaller percentage difference in the value of the failure pressure burst test and complex-shaped defect.

REFERENCES

1. DNV-RP-F101 (2004). *Corroded Pipelines, Subsea Pipeline and Risers, Norway: Det Norske Veritas*.
2. Arumugam, T., Karuppanan, S. and Ovinis, M. (2020) 'Finite element analyses of corroded pipeline with single defect subjected to internal pressure and axial compressive stress,' Malaysia: Mechanical Engineering Department, Universiti Teknologi PETRONAS
3. Mokhtari, M. and Melchers, R. E. (2018) 'A new approach to assess the remaining strength of corroded steel pipes,' Engineering Failure Analysis. Australia: Centre for Infrastructure Performance and Reliability, The University of Newcastle.
4. Al-Owaisi, S. et al. (2018) 'An experimental investigation of the effect of defect shape and orientation on the burst pressure of pressurized pipes,' Nottingham UK: College of Engineering, Mechanical and Industrial Engineering Department, Faculty of Engineering, University of Nottingham.
5. Al-Owaisi, S. S., Becker, A. A. and Sun, W. (2016) 'Analysis of shape and location effects of closely spaced metal loss defects in pressurized pipes,' Nottingham UK: College of Engineering, Mechanical and Industrial Engineering Department, Faculty of Engineering, University of Nottingham
6. Bao, J. et al. (2018) 'Evaluation of burst pressure of corroded pipe segments using three- Dimensional finite element analyses', Proceedings of the Biennial International Pipeline Conference, IPC